Characterization of human thioredoxin-like-1: Potential involvement in the cellular response against glucose deprivation

Alberto Jiménez[1,2], Markku Pelto-Huikko[3], Jan-Åke Gustafsson[1] and Antonio Miranda-Vizuete[1,4,5].

[1]Center for Biotechnology, Department of Biosciences at NOVUM, Karolinska Institutet, S-14157 Huddinge, Sweden.
[2]Instituto de Microbiología Bioquímica y Departamento de Microbiología y Genética, CSIC/Universidad de Salamanca, Campus Miguel de Unamuno, 37007 Salamanca, Spain.
[3]Department of Developmental Biology, Tampere University Medical School and Department of Pathology, Tampere University Hospital, Fin-33101 Tampere, Finland.
[4]Centro Andaluz de Biología del Desarrollo (CABD-CSIC), Departamento de Ciencias Ambientales, Universidad Pablo de Olavide, 41013 Sevilla, Spain.

[5]To whom correspondence should be addressed: amirviz@upo.es
Phone: +34 954 349381
Fax: +34 954 349376

Abbreviations: DTT, dithiothretitol; GST, glutathione-S-transferase; MTT, 3-[4,5-Dimethylthiazol- 2-yl]-2,5-diphenyltetrazolium bromide; Trx, thioredoxin; TrxR, thioredoxin reductase; Txl, thioredoxin-like; HEK, Human Embryonic Kidney

ABSTRACT

The thioredoxin system, composed of thioredoxin and thioredoxin reductase, emerges as one of the most important thiol-based systems involved in the maintenance of the cellular redox balance. Thioredoxin-like-1 (TXL-1) is a highly conserved protein comprising an N-terminal thioredoxin domain and a C-terminal domain of unknown function. Here we show that TXL-1 is a substrate for the cytosolic selenoprotein thioredoxin reductase. *In situ* hybridization experiments demonstrates high expression of *Txl-1* mRNA in various areas of central nervous system and also in some reproductive organs. Glucose deprivation, but not hydrogen peroxide treatment, reduced the levels of endogenous TXL-1 protein in HEK-293 cell line. Conversely, overexpression of TXL-1 protects against glucose deprivation-induced cytotoxicity. Taken together, the finding that *Txl-1* mRNA is highly expressed in tissues which use glucose as a primary energy source and the modulation of TXL-1 levels upon glucose deprivation indicate that TXL-1 might be involved in the cellular response to sugar starvation stress.

INTRODUCTION

The thioredoxin family encompasses a group of redox proteins that function as general protein disulphide reductases [8] participating in many physiological and pathophysiological processes [1,5]. The redox activity of thioredoxins (Trx) is directly linked to their highly conserved active site (Cys-Gly-Pro-Cys) where the cysteine residues can undergo a reversible oxidation from a dithiol to a disulphide form. Oxidized inactive forms are reduced by the selenoprotein thioredoxin reductase (TrxR), which uses the reducing power of NADPH [9]. Thioredoxins share a common globular structure consisting of a central core of β-sheets surrounded by α-helixes with the active site situated in a protrusion of the protein surface [12].

Different forms of thioredoxins have been reported in all organisms from prokaryotes to humans. In eukaryotic organisms thioredoxins are located in different subcellular compartments and are found either ubiquitously expressed or specifically localized in particular tissues [2,8,11,17,20,21,23]. Some of the previously described thioredoxins comprise additional domains with known or unknown counterparts in the databases [2,17,21,22,26,27].

Thioredoxin-like 1 (TXL-1), also known as TRP32 [17,21] is a two-domain protein of 32 kDa composed of a N-terminal thioredoxin domain followed by a C-terminal domain of unknown function with no homology with any other protein in the databases. *TXL-1* mRNA is ubiquitously localized in all human tissues examined so far, although it is present at highest levels in tissues with an elevated metabolic rate [17,21]. The crystal structure of the TXL-1 N-terminal domain has been solved [14] and shows a monomeric structure, in contrast to the ubiquitous cytosolic TRX-1 which is dimeric in all crystal structures reported [37].

We report here novel features of human TXL-1 concerning its ability to serve as substrate for thioredoxin reductase, new insights into its tissue localization and, more importantly, that TXL-1 is involved in the cellular response to glucose deprivation.

MATERIAL AND METHODS

Materials: All media and supplements used for cell culture including glucose-free DMEM were purchased from Life Technologies. Bovine thioredoxin reductase was from IMCO (Sweden). pET-15b vector was obtained from Novagen and pGEX-4T-1 vector was from Amersham Biosciences. pCDNA-myc empty vector was a gift from Dr. Eckardt Treuter. Anti-myc monoclonal antibody was purchased from Invitrogen. H_2O_2, Trypan Blue and MTT reagents were obtained from Sigma-Aldrich.

Human TXL-1 protein expression and purification: The ORF encoding human TXL-1 was cloned into the *Bam*HI-*Eco*RI sites of the pGEX-4T-1 expression vector and used to transform *E. coli* HMS174(DE3). Induction and purification of the recombinant protein was achieved as previously reported [21]. Thrombin (5 units/mg of fusion protein) was used to remove the glutathione *S*-transferase domain by incubation overnight at 4°C. The resulting protein preparation was then subjected to ion exchange chromatography using a Resource Q column (Amersham Biosciences), and human TXL-1 was eluted as a single peak using a gradient of NaCl. Protein concentration was determined with the Bio-Rad protein assay kit (Bio-Rad) using BSA as a standard.

Enzymatic Activity Assays: Enzymatic activity of recombinant human TXL-1 was performed using two different assays. In the *DTT assay*, DTT is used as reducing agent and the assay was carried out as previously described [38]. In the *thioredoxin reductase assay*, recombinant TXL-1 activity was determined by its capability to reduce insulin disulfide bonds using NADPH as electron donor in the presence of calf thymus thioredoxin reductase-1. The activity assay was performed essentially as described elsewhere [33] but monitoring insulin precipitation at 600nm. In both cases, human TRX-1 was used as control.

Antibody production: Purified His-hTXL-1 [21] was used to immunize rabbits (Zeneca Research Biochemicals). After six immunizations, serum from rabbits was purified by ammonium sulfate precipitation. Affinity-purified antibodies were prepared as described [24] using the TXL-1 fragment from the GST-TXL-1 recombinant protein. The specificity of the antibodies was tested by western blot.

Immunodetection was performed with horseradish peroxidase-conjugated donkey anti-rabbit IgG diluted 1/5,000 following the ECL protocol (Amersham Biosciences). Additionally, affinity purified polyclonal rabbit anti-TXL-1 and the respective blocking peptide were purchased from Abgent (San Diego, USA) for immunocytochemistry.

In situ hybridization: Adult (NMRI, weighting 20-25 g) and embryonic (embryonic days E9 – E18; E1 = the day of copulation plug) mice were used. Adult animals were killed with carbon dioxide, the tissues and embryos were rapidly excised, and frozen on dry ice. The frozen tissues were sectioned with Microm HM-500 cryostat at 14 μm and mounted on Polylysine glass slides (Menzel, Braunschweig, Germany). The sections were stored at –20ºC until use. Three oligonucleotide probes directed against mouse and rat *Txl-1* mRNA (mouse nucleotides 189-222, 263-294 and 361-394, GeneBank accession number NM_016792) were used for *in situ* hybridization. The sequences exhibited less than 60% homology with other known genes in the GeneBank database. Several probes against non-related mRNAs with known expression patterns and with similar length and GC-content were used as controls. Addition of 100-fold excess of non-labeled probes quenched all signal. The *in situ* hybridization was carried out as described in detail previously [28].

Immunocytochemistry: For immunocytochemistry adult NMRI mice were perfused first with 20ml of physiological saline followed with 50ml of 4% paraformaldehyde in phosphate buffered saline (PBS, 0.1M, pH 7.3). The brains were excised and further immersed in the same fixative for 1 h. After cryoprotection with 20% sucrose the tissues were sectioned at 10μm in Microm 500HM cryostat. Sections were incubated with the antibody (dil. 1:100) overnight in PBS containing 1% BSA and 0.1% Triton X-100. Immunoreactivity was visualised with Vectastain Elite-kit (Vector Laboratories, Burlingame, Ca, USA) using nickel-intensified diaminobenzidine as a chromogen. Presaturation of the antibody with 40μg of the blocking peptide and omission of the primary or secondary antibodies abolished all staining. Sections were examined under a Nikon FXA microscope equipped with a PCO Sensicam digital camera (PCO, Kelheim, Germany) and the images were processed using Corel Draw software (Corel Corporation Ltd., Ontario, Canada).

Cell culture and transient transfections: HEK-293 cells were cultured at 37ºC in an atmosphere of 5% CO_2 in DMEM medium supplemented with 10% fetal bovine serum, 100 U/ml penicillin and 100 μg/ml streptomycin. Transfection experiments were carried out as described elsewhere [13].

Stable transfection of HEK-293 cells: Plasmids pCDNA-myc and pCDNA-myc/TXL-1 were transfected into HEK-293 cells. Selection for G418 resistance (1 mg/ml) was initiated 48h after transfection and individual clones were isolated to obtain three different stable cell lines: control clone transfected with empty pCDNA-myc vector and two clones transfected with pCDNA-myc/TXL-1 showing different TXL-1 expression levels. TXL-1 overexpression was confirmed by western-blot analysis using anti-myc (not shown) and anti-TXL-1 antibodies.

MTT cell viability assay: Cell viability was assessed by MTT assay [25] that detects the cellular ability to transform MTT tetrazolium salt into formazan. MTT (0.3 mg/ml in DMEM without phenol red) was added to the cells. After 1 h incubation at 37ºC, the medium was removed and the formazan crystals were dissolved in the same volume of isopropanol. Aliquots were transferred to 96-well plates and the absorbance was measured at 540nm. Results were expressed as a percentage of viable cells.

Statistical analysis: Analyses of differences were carried out by ANOVA followed by the Student-Newman-Keuls post-hoc test. A value of $p<0.05$ was considered statistically significant.

RESULTS

Txl-1 is a two-domain protein conserved from fission yeast to humans

A protein-protein BLASTp search was performed to identify human TXL-1 orthologues in the public databases (http://www.ncbi.nlm.nih.gov/BLAST/), which resulted in several entries from the fission yeast to mammals. All these sequences were run on a W-Clustal alignment using the MegAlign program included in the DNAstar software package (Supplemental Data Fig. 1). Txl-1 protein is well conserved from lower eukaryotes to humans and the high identity is not only confined to the thioredoxin domain, but being comparable all along the protein sequence. All the Txl-1 proteins analyzed are about the same length (290 residues) and contain many of the amino acid residues identified as essential for catalysis, maintenance of three-dimensional structure or protein-protein interactions in previously characterized thioredoxins [3].

As mentioned above, Txl-1 is a two-domain protein with an N-terminal thioredoxin domain and a C-terminal domain with unknown function [17,21]. Nonetheless, the examination of the Conserved Domain Database at NCBI (http://www.ncbi.nlm.nih.gov/Structure/cdd/cdd.shtml) showed that two other classes of proteins different than Txl-1 contain a homologous domain, which is named Domain of Unknown Function 1000 (DUF1000). These two classes of proteins are the eukaryotic HT014 proteins, which comprise a unique DUF1000 domain, and the *Caenorhabditis elegans* ZK353.1 protein that encompasses a Cyclin N-terminal domain (Cyclin box fold) and a C-terminal DUF1000 domain.

Human TXL-1 has reducing activity coupled to thioredoxin reductase

We have now purified a GST-TXL-1 recombinant protein and assayed the thrombin-cleaved TXL-1 in the DTT assay resulting in detectable enzymatic activity, as previously reported [17] (data not shown). Recombinant thrombin-cleaved TXL-1 protein also displayed thioredoxin reducing activity in the presence of calf thymus thioredoxin reductase and NADPH (Fig. 1). Remarkably, the kinetics of TRX-1 and TXL-1 are different. First, TRX-1 shows a 4-fold higher thioredoxin activity than TXL-1 at the same concentration. Second, TXL-1 activity is delayed in time when

compared to that of TRX-1. TXL-1 starts to show the enzymatic activity after 45 min of initiating the assay, when TRX-1 has already reached its maximal activity. This long latency phase explains the failure to detect thioredoxin reductase-dependent activity of TXL-1 in our previous report [21].

Txl-1 mRNA tissue distribution

With *in situ* hybridization in mice, high level of *Txl-1* mRNA could be seen in several areas in nervous system. Especially olfactory bulb, hippocampus, habenular nucleus, several hypothalamic (Fig. 2A) and brain stem nuclei and cerebellar cortex (Fig. 2B) showed high expression. In peripheral nervous system moderate expression was seen in the neurons of trigeminal and superior cervical ganglion (Fig. 2C). In reproductive organs high expression was seen in the granulosa cells of different size follicles in ovary, while interstitial tissue and corpora lutea showed low expression (Fig. 2D). In testis moderate signal was observed in most seminiferous tubules (Fig. 2E). In epididymis strong signal was present in the epithelium of the tubules (Fig. 2F). In prostate low signal was seen in the epithelium (Fig. 2G) and in seminal vesicle low expression was seen in the muscle layer. In immune system moderate levels of *Txl-1* mRNA were observed in thymus (Fig. 2H), spleen and lymph nodes. In kidney moderate expression was present in the cortex and outer medulla while inner medulla and pelvis were devoid of signal (Fig. 2I). In urinary bladder low signal was present in the epithelium whereas muscle layer was devoid of signal. In salivary gland and liver (Fig. 2J) moderate homogenous signal was present. Pituitary gland and adrenal gland (Fig. 2K) showed low signal while thyroid gland was devoid of signal. In heart (Fig. 2L) and striated muscle (Fig. 2M) expression of *Txl-1* mRNA was low. In skin low expression could be detected (Fig. 2M). Strong *Txl-1* mRNA expression was seen in the embryonic side of the E9 placenta, while maternal side showed low expression. In E9 fetus clear signal was seen in the neuroepithelium of developing neural tube (Fig. 2N). Most organs which express *Txl-1* mRNA in adults showed expression already during fetal development (data not shown).

Immunocytochemical localization of TXL-1 in brain

As the central nervous system is one of the organs showing high levels of *Txl-1* mRNA, we further analyzed the expression pattern of Txl-1 protein in mouse brain tissue by immunocytochemistry.

Txl-1 immunoreactivity could be seen in several brain areas. Strong staining was seen in e.g. cerebral and cerebellar cortex (Fig. 3A) and hypothalamus (Fig. 3B). In cerebellar Purkinje neurons strong nuclear staining was evident. Moderate to low labeling was seen in the cytoplasm (Fig. 3A). Large number of granular neurons showed strong nuclear labeling and weak cytoplasmic staining. Few granular neurons exhibited moderate cytoplasmic staining with weak or non-labeled nucleus (Fig. 3A). In hypothalamic arcuate nucleus both nuclear and cytoplasmic staining was seen in most of the labeled cells while in some on cytoplasmic staining was evident (Fig. 3B). No staining was seen in the presaturation control (Fig. 3C).

In addition, we clearly observed both nuclear and cytoplasmic localization of a TXL-1-GFP fusion protein (Supplemental Data Fig. 2). Although the nuclear staining is weaker than with a transfection control using the pEGFP-N3 empty vector expressing the GFP protein alone, a comparison with cells transfected with pEGFP-N3/SPTRX-2 that express the cytoplasmic-restricted sperm-specific thioredoxin 2 [26] allow us to unequivocally confirm the nuclear labeling of TXL-1-GFP fusion protein.

Glucose deprivation but not hydrogen peroxide affects TXL-1 expression levels in HEK-293 cells

Brain tissue is very sensitive to ischemia (i. e. hypoxia and glucose deprivation). In addition, glucose deprivation induces cell death through a mechanism where metabolic oxidative stress is involved [18,30,31]. We wanted to know whether TXL-1 might be involved in this mechanism and therefore we investigated TXL-1 expression in HEK-293 cells after glucose deprivation. First, we confirmed that glucose-deprivation, as reported for other cell lines [18,32], induces cell death in HEK-293 cells (Fig. 4, left panel). Cytotoxicity is evident after 24h of treatment, counting up to 60% of cell death after 48h. With regard to TXL-1 expression upon glucose deprivation, TXL-1 protein levels do not change until 32 h (not shown) and

decrease after 36 h when HEK-293 cells are cultured in glucose-free medium (Fig. 4, right panel). In contrast, glucose deprivation does not affect TRX-1 or actin protein levels up to 48h.

Glucose deprivation-induced cytotoxicity is mediated by the generation of reactive oxygen species such as hydrogen peroxide [30]. Based on our previous results, we reasoned that the downregulation of TXL-1 expression caused by glucose deprivation might be mediated by hydrogen peroxide. Therefore, we checked whether hydrogen peroxide by itself might trigger modifications on TXL-1 protein levels. As shown in Fig. 5, hydrogen peroxide induces HEK-293 cell death within 2 h, reaching only 50% survival after 6 h, but does not cause any change in the endogenous levels of TXL-1. Extended incubation times caused massive cell death without any change in the levels of TXL-1 (not shown).

TXL-1 overexpression protects against glucose deprivation induced cytotoxicity

Next we wanted to know if TXL-1 overexpression might abolish or delay the cell death induced by glucose deprivation in HEK-293 cells. For this purpose, we made stable cell lines overexpressing TXL-1 to check whether constitutively increased TXL-1 protein levels have a protective effect on glucose deprivation-induced cytotoxicity. As shown in Fig. 6 we managed to isolate two stable clones with different TXL-1 expression levels (TXL-1-6 and TXL-1-16, with high and low expression levels of recombinant TXL-1, respectively) and one stable cell line with the pCDNA-myc empty vector to be used as negative control. Our results indicate that increased levels of TXL-1 can protect against the cytotoxicity induced by 48 to 72 h of glucose deprivation (Fig. 6). Thus, TXL-1-6 clone that expresses high levels of TXL-1 protein shows a significant delay in cell death and a higher rate of survival (about 50% more living cells than the control) from 48 h to 72 h (Fig. 6). However, TXL-1-16 clone that expresses low levels of TXL-1 is as sensitive as the control. In contrast, TXL-1 overexpression does not exert any effect against hydrogen peroxide cytotoxicity (not shown).

Discussion

Oxidative stress is involved in the progression of many different diseases and it is characterized by the depletion of the general antioxidant systems leading to an alteration of the cellular redox status. Thus, the balance between ROS production and antioxidants determines the degree of oxidative stress [4]. Thioredoxins have emerged as an essential family of proteins directly related to the antioxidant cellular network [5]. Here we present novel features of one member of the thioredoxin family, thioredoxin-like-1.

Txl-1 is one of the best conserved members of the thioredoxin family. This fact probably implies an important function of this protein in the physiology of eukaryotic organisms. It is also remarkable that the active site of Txl-1 homologues in lower eukaryotes and invertebrates contains a tryptophan residue (WCGPC), as is also the case of most thioredoxins [10], while in Txl-1 from vertebrates, this tryptophan residue is substituted by a glycine residue (GCGPC). The presence of the bulky imidazole side chain of Trp31 has been proposed to regulate the catalytic activity of thioredoxins [16]. Indeed, we found that the thioredoxin activity kinetics are considerably different between TXL-1 and TRX-1, making it reasonable to speculate that the substitution of Trp31 to Gly31 might explain this difference. Nonetheless, the biological significance of this change requires further analysis.

High expression of *Txl-1* mRNA could be seen in tissues which mainly use glucose as an energy source and low expression in tissues which utilize fatty acids as energy supplier. This finding aimed us to further investigate the localization of Txl-1 in brain, which in normal situation relies solely on glucose. Our results show that Txl-1 can be seen either in the nucleus or the cytoplasm of different cells types in the brain (Fig. 3). In addition, a TXL-1-GFP fusion protein also displays both nuclear and cytoplasmic localization (Supplementary Data Fig. 2), thus confirming the TXL-1 subcellular localization pattern observed with immunocytochemistry. However, there is no nuclear targeting signal in the TXL-1 sequence. In close parallelism, TRX-1 can also translocate into the nucleus under certain conditions [7] without such targeting signal in its sequence. The roles of TRX-1 in nucleus and cytoplasm seem to be different [7,35] and it has been shown that nuclear TRX-1 modulates, in a redox-dependent manner, the DNA binding activity of transcription factors [15,36], including nuclear receptors [6,19]. Taken together, we may speculate that regulation of activity

of transcription factors might be one role of TXL-1 within the nucleus and that TXL-1 might be an important factor in protecting nervous system against the effects of hypoglycemia.

TXL-1 expression is clearly modulated by glucose deprivation in HEK-293 cells since TXL-1 protein levels are reduced after 36 h in this condition (see Fig. 5B). Unlike TXL-1, TRX-1 levels do not change after 48 h in a glucose-free medium. This result indicates that TXL-1 might be specifically involved in the cellular response to glucose deprivation. It is well accepted that glucose deprivation-induced cytotoxicity is mediated by the generation of ROS, e.g. hydrogen peroxide, that promotes the activation of the c-Jun N-terminal kinase (JNK-1) pathway through the disruption of the interaction between TRX-1 and the apoptosis signaling kinase-1 (ASK-1). The activation of this pathway leads to the progression of the apoptotic process and cell death [29-31]. However, TXL-1 expression is not affected by hydrogen peroxide exposure, so the effect of glucose deprivation on TXL-1 expression must be mediated through a different pathway where hydrogen peroxide is not involved.

We have also found that overexpression of TXL-1 over a certain threshold can protect HEK-293 cells against glucose deprivation cytotoxicity. Significant differences in cell survival appear after 48 h treatment when comparing clones with highest TXL-1 levels. Before 36 h, cell survival is comparable in all clones, most probably because TXL-1 levels are high enough to maintain the cellular integrity. However, after 36 h and onwards only the TXL-1-6 clone showing the highest expression level is able to protect cells to some extent from glucose deprivation-induced cytotoxicity. Again, hydrogen peroxide-induced cytotoxicity is not prevented by TXL-1 overexpression supporting our previous idea that TXL-1 must function in a pathway where hydrogen peroxide is not involved.

In summary, we propose TXL-1 to be involved in the cellular response against glucose deprivation. However, more experiments are required to elucidate the specific mechanism and the molecular targets of TXL-1 in this particular process.

Acknowledgements

This work was supported by the Swedish Medical Research Council (projects 03P-14096, 03X-14041, and 13X-10370), the Åke Wibergs Stiftelse, the Karolinska Institutet and Medical Research Fund of Tampere University Hospital,. A. Jiménez was supported by a postdoctoral fellowship (EX2003-0390) from the Spanish Ministerio de Educación, Cultura y Deporte. We thank Sergio J. Montaño for excellent technical assistance in the preparation of TXL-1 stable clones and Mrs. Ulla Jukarainen for technical assistance with *in situ* hybridizations.

References

[1] Arner, E.S. and Holmgren, A. (2000) Physiological functions of thioredoxin and thioredoxin reductase Eur J Biochem 267, 6102-9.

[2] Cunnea, P.M. et al. (2003) ERdj5, an endoplasmic reticulum (ER)-resident protein containing DnaJ and thioredoxin domains, is expressed in secretory cells or following ER stress J Biol Chem 278, 1059-66.

[3] Eklund, H., Gleason, F.K. and Holmgren, A. (1991) Structural and functional relations among thioredoxins of different species. Proteins: Structure, function and genetics 11, 13-28.

[4] Finkel, T. and Holbrook, N.J. (2000) Oxidants, oxidative stress and the biology of ageing Nature 408, 239-47.

[5] Gromer, S., Urig, S. and Becker, K. (2004) The thioredoxin system-From science to clinic Med Res Rev 24, 40-89.

[6] Hayashi, S., Hajiro-Nakanishi, K., Makino, Y., Eguchi, H., Yodoi, J. and Tanaka, H. (1997) Functional modulation of estrogen receptor by redox state with reference to thioredoxin as a mediator Nucleic Acids Res 25, 4035-40.

[7] Hirota, K., Murata, M., Sachi, Y., Nakamura, H., Takeuchi, J., Mori, K. and Yodoi, J. (1999) Distinct roles of thioredoxin in the cytoplasm and in the nucleus. A two-step mechanism of redox regulation of transcription factor NF-kappaB J Biol Chem 274, 27891-7.

[8] Hirota, K., Nakamura, H., Masutani, H. and Yodoi, J. (2002) Thioredoxin superfamily and thioredoxin-inducing agents Ann N Y Acad Sci 957, 189-99.

[9] Holmgren, A. (2000) Antioxidant function of thioredoxin and glutaredoxin systems Antioxid Redox Signal 2, 811-20.

[10] Holmgren, A. and Björnstedt, M. (1995) Thioredoxin and thioredoxin reductase Methods Enzymol. 252, 199-208.

[11] Hosoda, A., Kimata, Y., Tsuru, A. and Kohno, K. (2003) JPDI, a novel endoplasmic reticulum-resident protein containing both a BiP-interacting J-domain and thioredoxin-like motifs J Biol Chem 278, 2669-76.

[12] Jeng, M.F., Campbell, A.P., Begley, T., Holmgren, A., Case, D.A., Wright, P.E. and Dyson, H.J. (1994) High-resolution solution structures of oxidized and reduced Escherichia coli thioredoxin Structure 2, 853-68.

[13] Jimenez, A. et al. (2004) Spermatocyte/spermatid-specific thioredoxin-3, a novel Golgi apparatus-associated thioredoxin, is a specific marker of aberrant spermatogenesis J Biol Chem 279, 34971-82.

[14] Jin, J. et al. (2002) Crystal structure of the catalytic domain of a human thioredoxin-like protein Eur J Biochem 269, 2060-8.

[15] Khomenko, T., Deng, X., Jadus, M.R. and Szabo, S. (2003) Effect of cysteamine on redox-sensitive thiol-containing proteins in the duodenal mucosa Biochem Biophys Res Commun 309, 910-6.

[16] Krause, G. and Holmgren, A. (1991) Substitution of the conserved tryptophan 31 in Escherichia coli thioredoxin by site-directed mutagenesis and structure-function analysis J Biol Chem 266, 4056-66.

[17] Lee, K.-K., Murakawa, M., Takahashi, S., Tsubuki, S., Kawashima, S., Sakamaki, K. and Yonehara, S. (1998) Purification, molecular cloning and characterization of TRP32, a novel thioredoxin-related mammalian protein of 32 kDa J. Biol. Chem. 273, 19160-19166.

[18] Lee, Y.J., Galoforo, S.S., Berns, C.M., Chen, J.C., Davis, B.H., Sim, J.E., Corry, P.M. and Spitz, D.R. (1998) Glucose deprivation-induced cytotoxicity

and alterations in mitogen-activated protein kinase activation are mediated by oxidative stress in multidrug-resistant human breast carcinoma cells J Biol Chem 273, 5294-9.

[19] Makino, Y., Yoshikawa, N., Okamoto, K., Hirota, K., Yodoi, J., Makino, I. and Tanaka, H. (1999) Direct association with thioredoxin allows redox regulation of glucocorticoid receptor function J Biol Chem 274, 3182-8.

[20] Miranda-Vizuete, A., Damdimopoulos, A.E. and Spyrou, G. (2000) The mitochondrial thioredoxin system Antioxid Redox Signal 2, 801-10.

[21] Miranda-Vizuete, A., Gustafsson, J.-Å. and Spyrou, G. (1998) Molecular cloning and expression of a cDNA encoding a human thioredoxin-like protein Biochem. Biophys. Res. Commun 243, 284-288.

[22] Miranda-Vizuete, A., Ljung, J., Damdimopoulos, A.E., Gustafsson, J.A., Oko, R., Pelto-Huikko, M. and Spyrou, G. (2001) Characterization of Sptrx, a novel member of the thioredoxin family specifically expressed in human spermatozoa J Biol Chem 276, 31567-74.

[23] Miranda-Vizuete, A., Sadek, C.M., Jimenez, A., Krause, W.J., Sutovsky, P. and Oko, R. (2004) The Mammalian testis-specific thioredoxin system Antioxid Redox Signal 6, 25-40.

[24] Miranda-Vizuete, A., Tsang, K., Yu, Y., Jimenez, A., Pelto-Huikko, M., Flickinger, C.J., Sutovsky, P. and Oko, R. (2003) Cloning and Developmental Analysis of Murid Spermatid-specific Thioredoxin-2 (SPTRX-2), a Novel Sperm Fibrous Sheath Protein and Autoantigen J Biol Chem 278, 44874-85.

[25] Mosmann, T. (1983) Rapid colorimetric assay for cellular growth and survival: application to proliferation and cytotoxicity assays J Immunol Methods 65, 55-63.

[26] Sadek, C.M., Damdimopoulos, A.E., Pelto-Huikko, M., Gustafsson, J.J., Spyrou, G. and Miranda-Vizuete, A. (2001) Sptrx-2, a fusion protein composed of one thioredoxin and three tandemly repeated NDP-kinase domains is expressed in human testis germ cells Genes Cells 6, 1077-1090.

[27] Sadek, C.M. et al. (2003) Characterization of human thioredoxin-like 2 (Txl-2): a novel microtubule-binding thioredoxin predominantly expressed in the cilia of lung airway epithelium and spermatid manchette and axoneme J Biol Chem.

[28] Schultz, R., Suominen, J., Varre, T., Hakovirta, H., Parvinen, M., Toppari, J. and Pelto-Huikko, M. (2003) Expression of aryl hydrocarbon receptor and aryl hydrocarbon receptor nuclear translocator messenger ribonucleic acids and proteins in rat and human testis Endocrinology 144, 767-76.

[29] Song, J.J. and Lee, Y.J. (2003) Catalase, but not MnSOD, inhibits glucose deprivation-activated ASK1-MEK-MAPK signal transduction pathway and prevents relocalization of Daxx: hydrogen peroxide as a major second messenger of metabolic oxidative stress J Cell Biochem 90, 304-14.

[30] Song, J.J. and Lee, Y.J. (2003) Differential role of glutaredoxin and thioredoxin in metabolic oxidative stress-induced activation of apoptosis signal-regulating kinase 1 Biochem J 373, 845-53.

[31] Song, J.J. and Lee, Y.J. (2003) Effect of glucose concentration on activation of the ASK1-SEK1-JNK1 signal transduction pathway J Cell Biochem 89, 653-62.

[32] Spitz, D.R., Sim, J.E., Ridnour, L.A., Galoforo, S.S. and Lee, Y.J. (2000) Glucose deprivation-induced oxidative stress in human tumor cells. A fundamental defect in metabolism? Ann N Y Acad Sci 899, 349-62.

[33] Spyrou, G., Enmark, E., Miranda-Vizuete, A. and Gustafsson, J.-Å. (1997) Cloning and expression of a novel mammalian thioredoxin J. Biol. Chem. 272, 2936-2941.
[34] Thompson, J.D., Higgins, D.G. and Gibson, T.J. (1994) CLUSTAL W: improving the sensitivity of progressive multiple sequence alignment through sequence weighting, position-specific gap penalties and weight matrix choice Nucleic Acids Res 22, 4673-80.
[35] Watson, W.H. and Jones, D.P. (2003) Oxidation of nuclear thioredoxin during oxidative stress FEBS Lett 543, 144-7.
[36] Wei, S.J. et al. (2000) Thioredoxin nuclear translocation and interaction with redox factor-1 activates the activator protein-1 transcription factor in response to ionizing radiation Cancer Res 60, 6688-95.
[37] Weichsel, A., Gasdaska, J.R., Powis, G. and Montfort, W.R. (1996) Crystal structures of reduced, oxidized and mutated human thioredoxins: evidence for a regulatory homodimer. Structure 4, 735-751.
[38] Wollman, E. et al. (1988) Cloning and expression of a cDNA for human thioredoxin J. Biol. Chem. 263, 15506-15512.

Figure Legends

Fig. 1. Reducing activity of human TXL-1. TRX-1 (●) and purified TXL-1 (▲, 10μg; □, 20μg) were assayed for their ability to reduce insulin disulfide bonds in the presence of NADPH and calf thymus thioredoxin reductase (TrxR-1). Reactions with TrxR-1 alone (O) served as controls. A total of 1μg of TrxR-1 was used in each reaction. Identical results were obtained from three independent experiments.

Fig. 2. Localization of *Txl-1* mRNA in mouse tissues with *in situ* hybridization. High expression of *Txl-1* mRNA can be seen in the hippocampus (hc) and the hypothalamus (hy). Arrowheads show arcuate nucleus of hypothalamus and arrows point to habenular nucleus. Cerebral cortex (co) exhibits moderate signal (**A**). Strong signal is present in the granular cell layer of cerebellar cortex (co) and some nuclei of brain stem (bs) (**B**). Neurons (arrowheads) of trigeminal ganglion show moderate expression (**C**). In ovary prominent signal is seen in different size follicles (arrowheads) while interstitial tissue (it) shows low expression (**D**). Most of the seminiferous tubules (arrowheads) of testis exhibit moderate signal (**E**). The epithelium of the tubules (arrowheads) of epididymis shows strong signal (**F**). Low signal is present in the epithelium (arrowheads) in prostate (**G**). Moderate expression is seen throughout the thymus (**H**). In kidney moderate signal is present in cortex (co) and outer medulla (om) while inner medulla (im) and renal pelvis are non-labelled (**I**).

Homogenous expression can be seen liver (**J**). Low expression is present in adrenal cortex (co) and medulla (me) (**K**). In heart very low signal is in heart muscle (**L**). In skeletal muscle (mu) of tongue low signal is present and the epithelium (arrowheads) shows somewhat stronger signal (**M**). In placenta (pl) strong signal is seen in the fetal part (arrowheads) while maternal part and uterus (triangels) shows low expression. Clear signal is present in the neuroepithelium (arrow) of neural tube of E9 fetus (**N**). Bar in A represent 210 μm (A, F), 230 μm (B), 100 μm (C, E, G), 180 μm (D, H, I, L), 35 μm (J), 65 μm (K), 90 μm (M) and 240 μm (N).

Fig. 3. Immunolocalization of Txl-1 in brain tissue. A, Txl-1 immunoreactivity in cerebellar cortex. Strong nuclear (arrow) and moderate cytoplasmic staining (arrowheads) can be seen in the Purkinje cell (pc). Large number of granular

neurons (gc) show strong nuclear and moderate cytoplasmic labeling (arrows) while few exhibit only moderate cytoplasmic staining (double arrowheads) (mc, molecular layer). **B**, Txl-1 immunoreactivity in hypothalamic arcute nucleus. Some neurons show clear cytoplasmic staining with low nuclear labeling (arrowheads) while other neurons exhibit strong nuclear labeling (arrows). **C**, presaturation control of the adjacent section to B, no staining can be seen in the control. Bar in A represents 30μm for A-C.

Fig. 4. Effect of glucose deprivation on HEK-293 cells and TXL-1 protein levels. Left panel, HEK-293 cells were cultured in a glucose-free medium during 48 h. Cell survival was calculated using the MTT assay and it is represented as a percentage of living cells compared with HEK-293 cells grown in medium with glucose. Right panel, HEK-293 cells were cultured in a glucose-containing medium and a glucose-free medium during 48 h. Cell lysates (25μg) from representative time-points were separated by SDS-PAGE and immunoblotted with anti-TXL-1, anti-TRX-1 and anti-β-actin.

Fig. 5. Effect of hydrogen peroxide on HEK-293 cells and TXL-1 protein levels. Right panel, HEK-293 cells were cultured in the presence of 0.5mM H_2O_2 during 6 h. Cell survival was calculated using the Trypan Blue exclusion assay. Left panel, crude protein extracts (25μg) from HEK-293 cells treated (0-6 h) with 0.5mM H_2O_2 were subjected to western-blot analysis using the anti-TXL-1 and anti-β-actin antibodies.

Fig. 6. Overexpression of TXL-1 protects HEK-293 cells against glucose deprivation-induced cytotoxicity. Upper panel, cell lysates (25μg) from non transfected (n. t.) HEK-293 cells or cells transfected with empty pCDNA-myc or pCDNA-myc/TXL-1 (clones 6 and 16) were separated by SDS-PAGE and immunoblotted with anti-TXL-1 and anti-β-actin. Extracts from TXL-1-6 and TXL-1-16 clones show two bands with anti-TXL-1 antibody corresponding to the endogenous TXL-1 (lower band) and the myc-TXL-1 (upper band). Lower panel, cell viability MTT assay of HEK-293 stably transfected cells (TXL-1-6 and TXL-1-16) compared with HEK-293 cells stably transfected with the empty pCDNA-myc vector. Bars indicate

mean ± SEM with data expressed as percentage of living cells. Comparisons among clones were performed using ANOVA followed by the Student-Newman-Keuls post-hoc test (N=8, $P<0.05$). Statistical significant differences are indicated with an asterisk.

Supplemental Data Fig. 1. Sequence comparison of Txl-1 proteins from several representative eukaryotic species. The alignment was performed using the W-CLUSTAL program included in the DNAStar package [34]. Identical residues are shadowed, the thioredoxin domain is indicated with an arrow and the thioredoxin-active site is boxed.

Supplemental Data Figure 2. Subcellular localization of human TXL-1. A TXL-1-GFP construct transfected into HEK-293 cells shows green fluorescence in the nucleus and cytosol. pEGFP-N3 vector expressing GFP alone was transfected into HEK-293 cells as a control of nuclear and cytoplasmic staining. A SPTRX-2-GFP construct was used as a cytoplasmic control in the same HEK-293 cells. All micrographs were obtained from a single focal section.

Figure 1

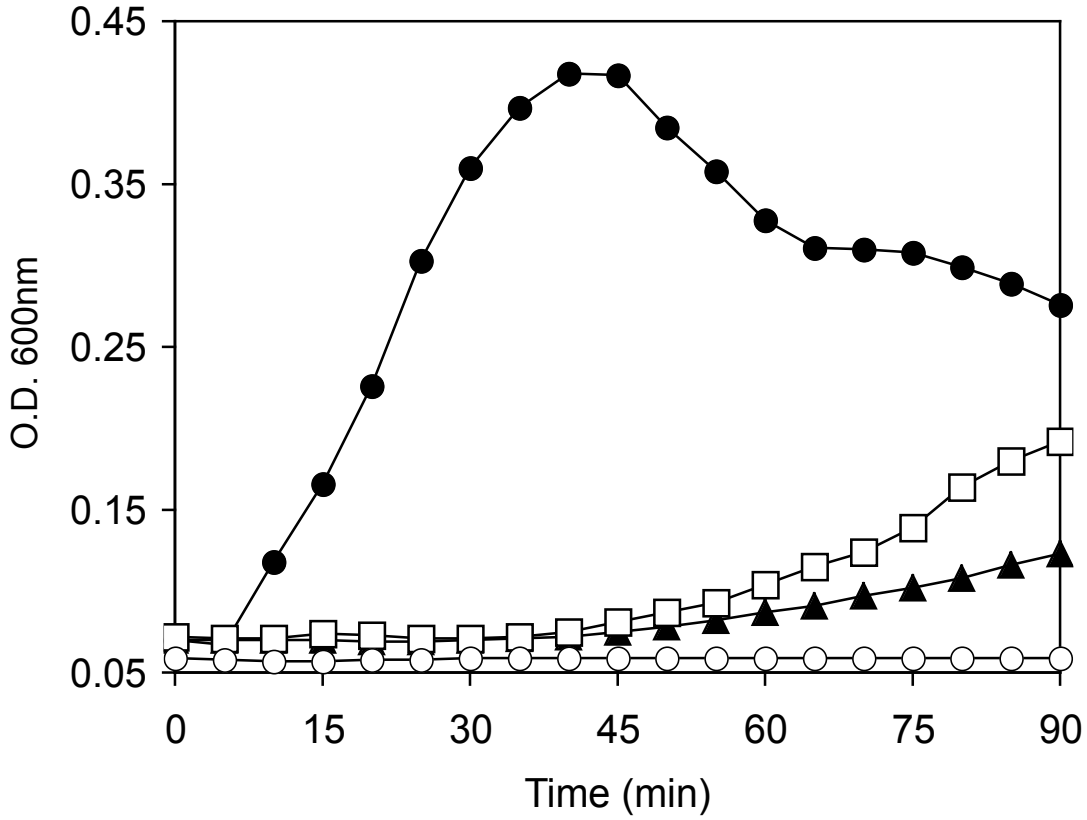

Figure 1

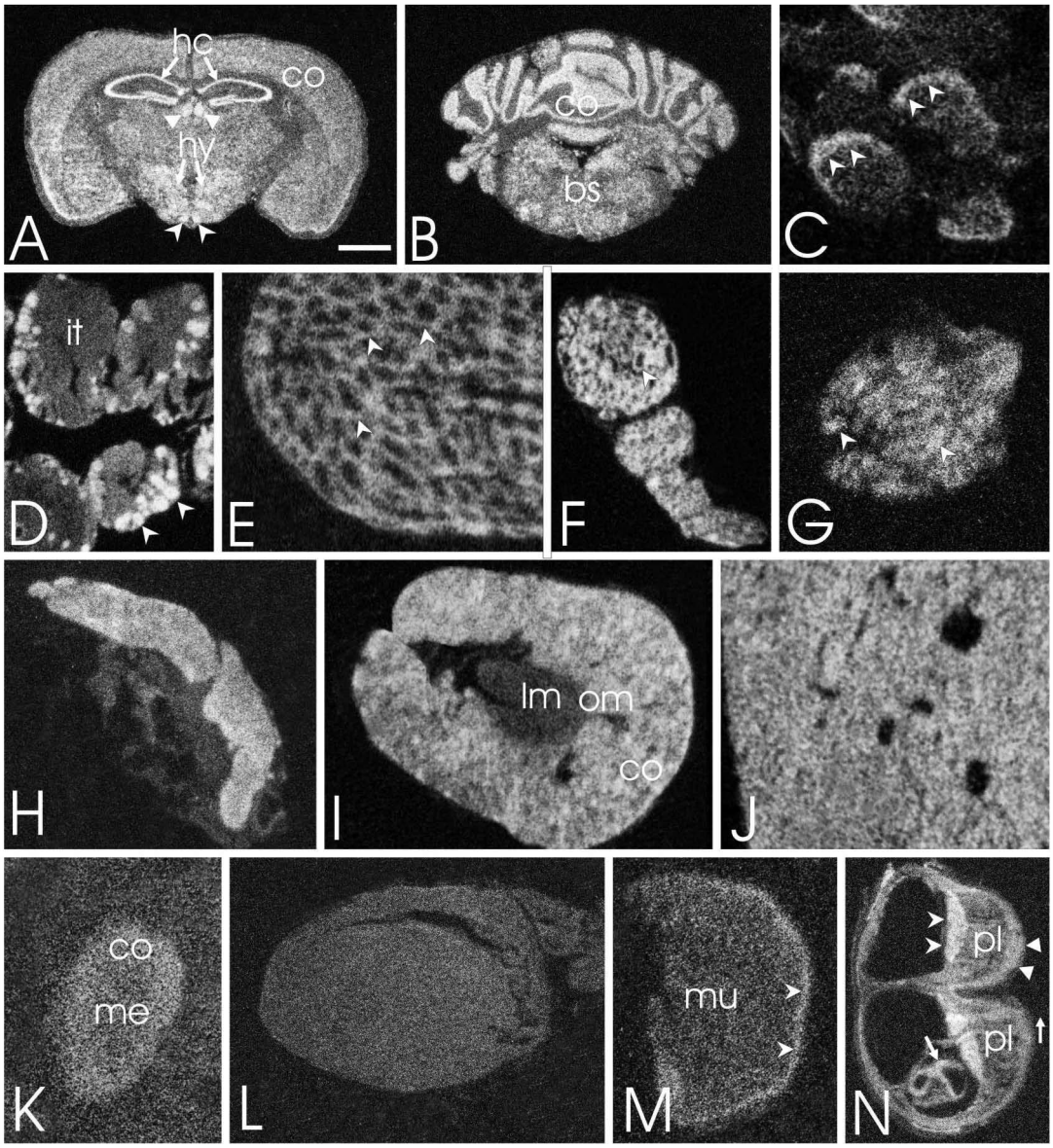

Figure 2

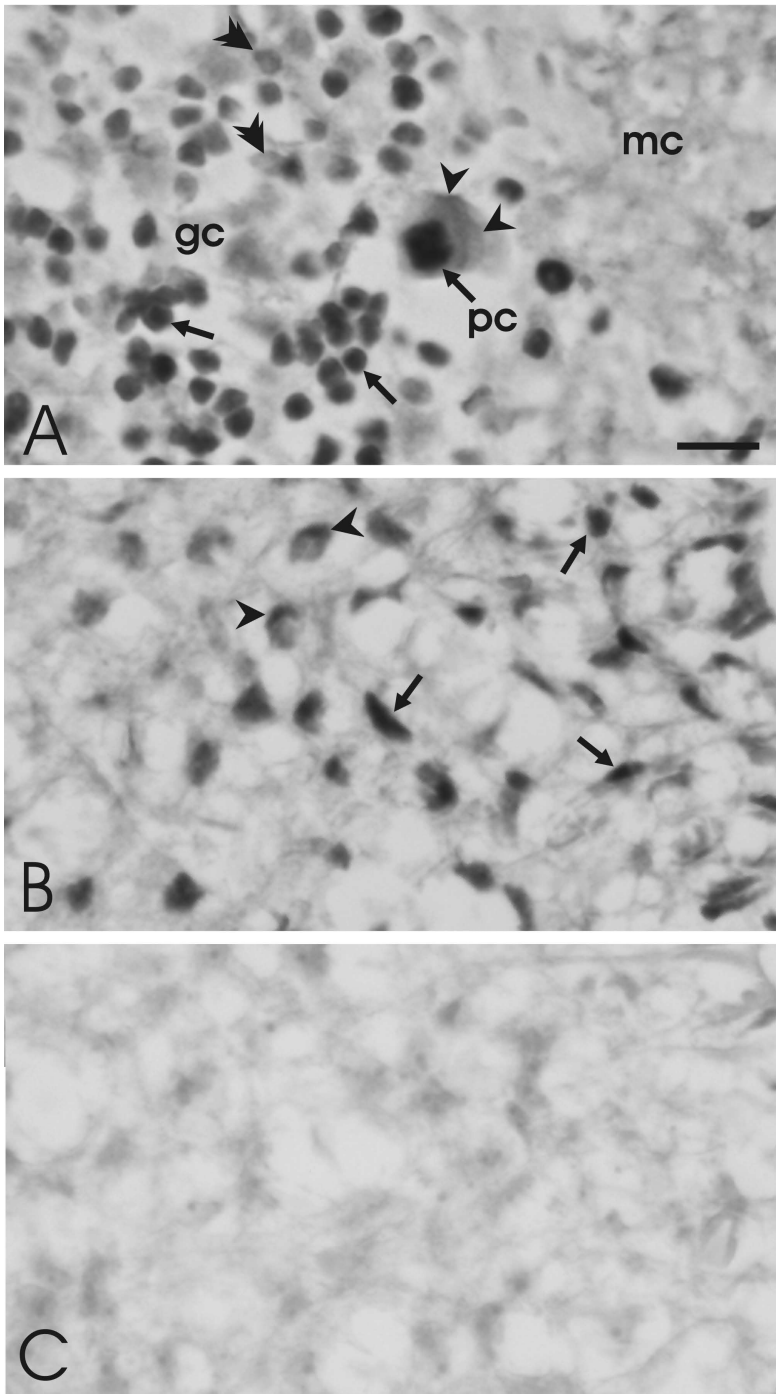

Figure 3

Figure 4

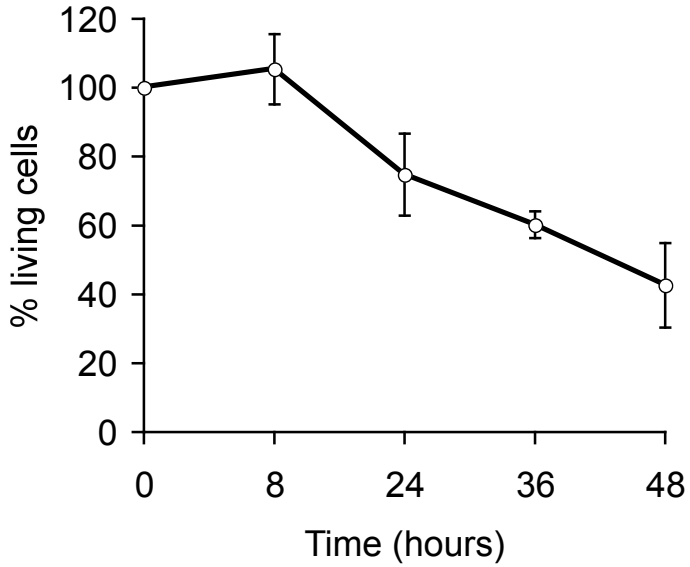

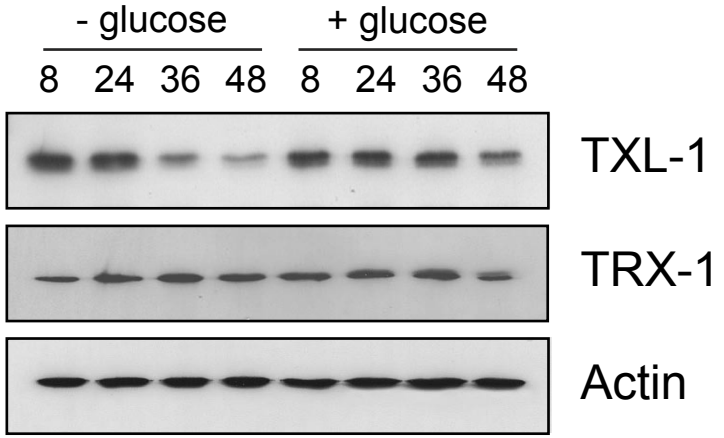

Figure 4

Figure 5

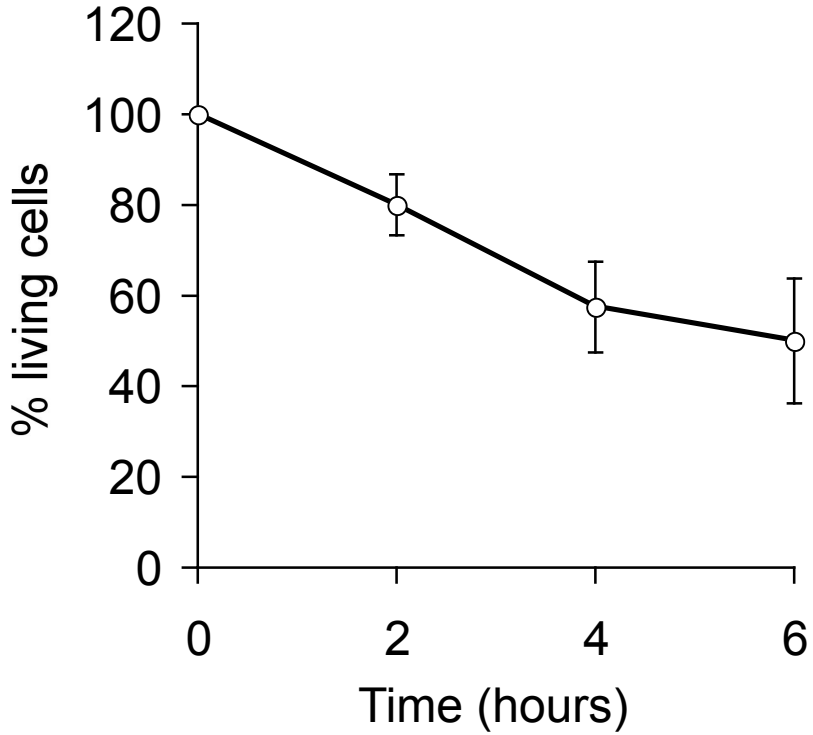

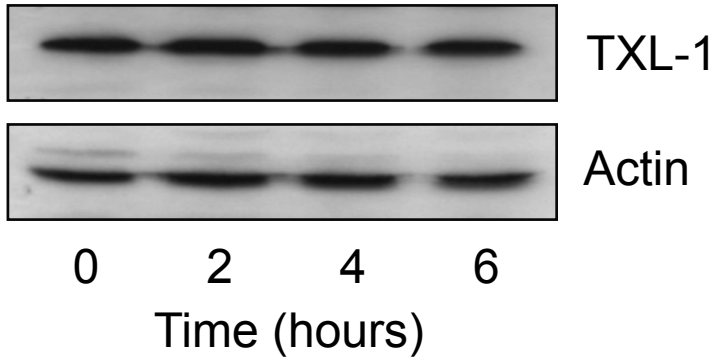

Figure 5

Figure 6

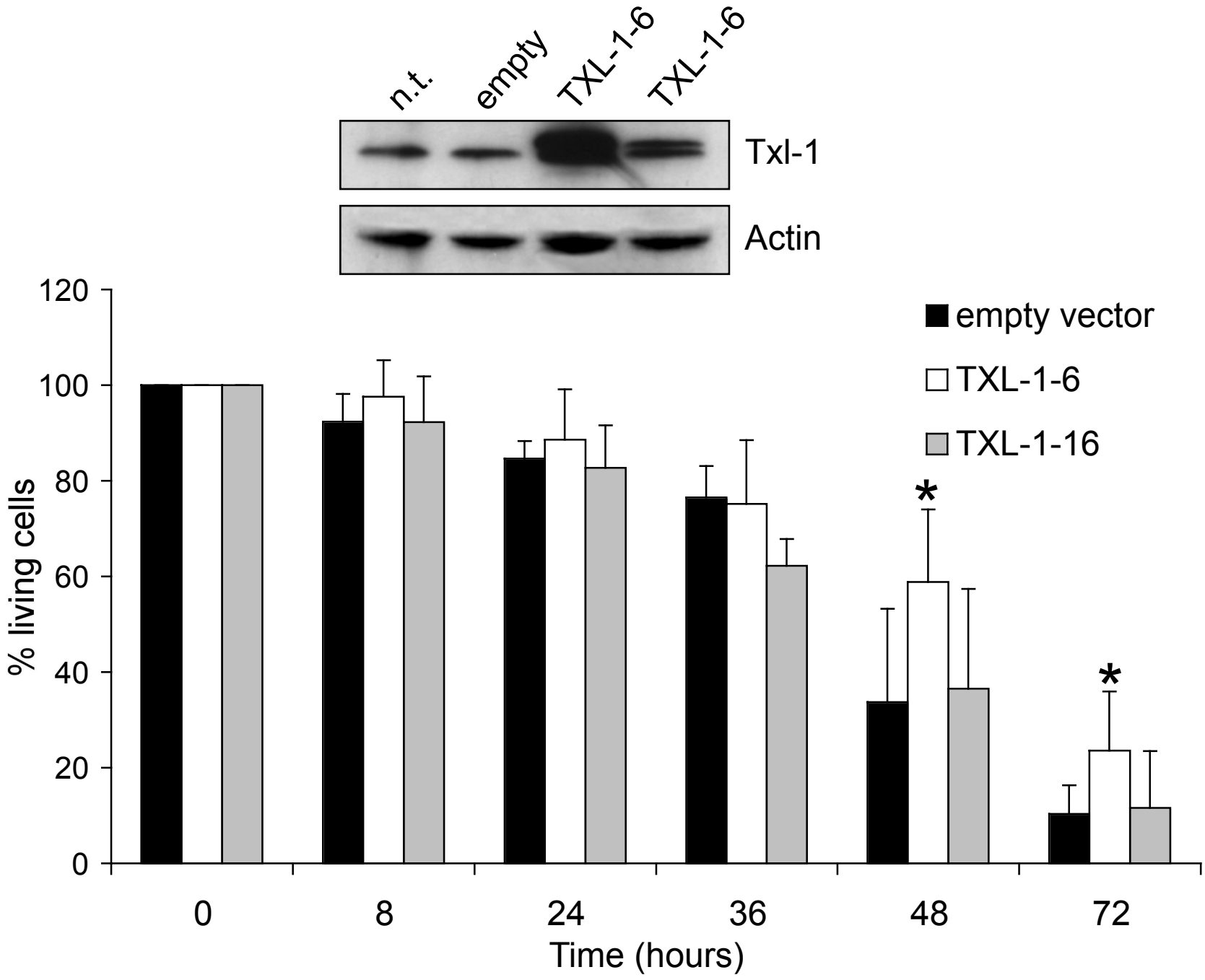

Figure 6

Supplementary Data 1

Click here to download Supplementary Data: Supplemental Data Figure 1.pdf

Supplementary Data 2

Click here to download Supplementary Data: Supplemental Data Figure 2.pdf